THE JOURNAL OF PHYSICAL CHEMISTRY B

Article

pubs.acs.org/JPCB

Excluded Volume Effect in the Fluorescence Energy Transfer of Single Donor−Multiple Acceptors in Polymer

Hyemin Lee and Minyung Lee*

Department of Chemistry and Nanoscience, Ewha Womans University, Seoul 120-750, Republic of Korea

ABSTRACT: Fluorescence resonance energy transfer (FRET) from a donor to multiple acceptors is an interesting subject. Numerous studies using theoretical models and simulations have focused on the excluded volume effect, which was not considered in Förster's first derivation. In this work, we first present the experimental results on the excluded volume effect by employing time-resolved FRET. Coumarin 334 (C334) was used as the energy donor whereas hemin and cytochrome *c* (cyt *c*) were used as the energy acceptors. The fluorescence intensity decays were measured for C334 surrounded by a number of acceptors in poly(acrylic acid). We have observed that the excluded volume effect is markedly pronounced with cyt *c* compared with hemin when the acceptor concentration is high (>5 mM). The results, which may be explicitly described by the relative molecular sizes of two acceptors, showed that the excluded volume effect should be considered in the interpretation of FRET data, especially when bulk chromophores are used.

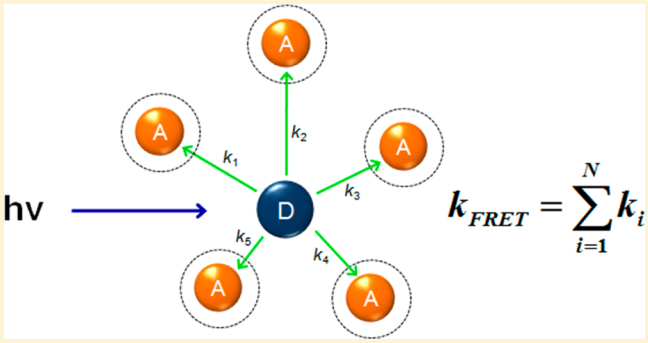

INTRODUCTION

Fluorescence resonance energy transfer (FRET) basically occurs through a (transition) dipole−dipole interaction between an excited donor (D) and a ground-state acceptor (A) at a length scale of 1−10 nm.[1,2] When τ_D is the fluorescence lifetime of a donor molecule in the absence of acceptors, the fluorescence lifetime in the presence of acceptors (τ_{DA}) is shortened due to FRET:

$$\tau_{DA} = \frac{1}{k_D + k_T} \tag{1}$$

where $k_D = 1/\tau_D$ and k_T is the energy transfer rate constant. The rate constant k_T depends on the spectral overlap between donor emission and acceptor absorption, relative transition dipole orientations (because there are many acceptors), and D−A distances. The rate constant is time-independent when the chromophores are embedded in a rigid matrix where they are translationally and rotationally immobile. In this case, the static averaging is more appropriate than the dynamic averaging.[3,4] An ensemble system in which donors and acceptors are randomly distributed in a matrix can be considered as a special case that involves several FRET processes such as D−D, D−A, and A−A transitions. The D−D and A−A transitions are known as a homo-FRET and the D−A transition is a hetero-FRET. The full analysis covering those processes are quite complex. A simple model can be set with low donor concentration and short acceptor lifetime. Then, the energy-transfer process (hetero-FRET) of a donor to multiple acceptors can be effectively monitored.

Förster first derived a donor ensemble decay function of such a system:[1]

$$I(t) = \exp[-(at + bt^{1/2})] \tag{2}$$

with

$$a = k_D, \quad b = \frac{4}{3}\pi^{3/2} n_A R_0^{\,3} k_D^{\,1/2}$$

where n_A is the acceptor number density and R_0 is the Förster radius. This equation has been widely used to calculate the acceptor concentrations by fitting to the experimental decay curves.[3] However, the procedure may be problematic at the high concentration limit because the equation was derived without considering the excluded volume effect. In general, the energy-transfer process can be investigated using either steady-state or time-resolved fluorescence, which measures the intensity and fluorescence lifetime, respectively. The time-resolved method has an advantage over the intensity measurement in that it directly records the intensity decay process. The time−intensity profile, which is concentration-independent, contains valuable information on the D−A distance distribution. Such an advantage enables time-resolved fluorescence spectroscopy to be an increasingly important technique for FRET studies. In time-resolved FRET studies, eq 2 has been quite successful at low and moderate acceptor concentrations.[5,6] In spite of its importance, any experimental work on

Received: June 22, 2012
Revised: September 5, 2012
Published: September 11, 2012

the excluded volume effect has not yet been intensively pursued.

In this work, we have attempted to described the effect of excluded volume in the FRET process using time-resolved fluorescence measurements. We used coumarin 334 (C334) as the energy donor and hemin and cytochrome *c* (cyt *c*) as the energy acceptors. C334 is a derivative of 1,2-benzopyrone (coumarin) (Scheme 1). To improve the photostability and

Scheme 1. Molecular Structure of 1,2-Benzopyrone (Coumarin)

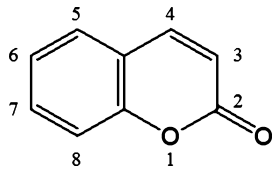

quantum yield, coumarin dyes are usually prepared as derivatives in which electron-donating groups are attached at the 4-, 5-, or 7-positions, while the carbonyl group at the 2-position acts as the electron acceptor.[7] The electron-accepting group can also be attached to the 3-, 6-, and 8-positions. Such coumarin derivatives have been widely used as laser dyes, solar cells, and fluorescent probes.[8−14] A recent study has suggested that coumarin analogues could be used as novel inhibitors of β-amyloid (Aβ) aggregation, which has been thought to be a main cause of Alzheimer' disease.[15] As an acceptor, hemin is an iron-containing porphyrin with a chloride axial ligand. Hemin is formed from degradation of hemoprotein in the presence of excess sodium chloride. As another acceptor, cyt *c* is one of the hemoproteins that has been widely used for FRET in bioscience. We used bovine heart cyt *c*, which consists of 104 amino acid residues. Considering the molecular structures of the two acceptors, they may serve as the basic structures of core and core−shell molecules in which cyt *c* has a chromophore (heme) enclosed within a peptide structure. We measured the intensity decays of C334 surrounded by a number of acceptors (hemin or cyt *c*) in poly(acrylic acid) (PAA) and observed that cyt *c* showed a pronounced excluded volume effect in comparison with hemin.

EXPERIMENTAL SECTION

Materials. Coumarin 334, hemin, cytochrome *c* (bovine heart), and poly(acrylic acid) (PAA) ($M_w \sim 240\,000$) were purchased from Sigma-Aldrich. The C334 dye was dissolved in water under sonication. The stock solutions of hemin and cyt *c* were prepared in DMSO and diluted with distilled water. Two sets of PAA solutions were prepared: for hemin, the PAA was dissolved in distilled water, and for cyt *c*, the PAA solution was neutralized to pH 7 with 3 M NaOH before use. Thin films were prepared by dropping each solution onto a cover glass. Those samples were desiccated at room temperature for 24 h to remove any remaining solvent.

Steady-State Measurements. The absorption spectra were obtained using a UV−visible spectrometer (UV-2450, Shimadzu). The fluorescence spectra were obtained using a spectrofluorometer (F-4500, Hitachi). Samples were Pt coated with a thickness of ∼3 nm, and the films thicknesses were obtained by scanning electron microscopy (SEM) (JSM-6700F, JEOL) at an accelerating voltage of 10 keV.

Time-Resolved Studies. The fluorescence lifetimes of C334 in the absence and presence of acceptors in the polymer films were measured by time-correlated single photon counting (TCSPC). The light source for sample excitation was a picosecond diode laser operating at a wavelength of 467 nm at 10 MHz (Picoquant, PDL 800-B). An inverted confocal microscope (Nikon, TE2000-S) with an oil immersion objective lens (NA 1.4, 60×) was used as a platform for sample excitation and fluorescence detection. A single-mode fiber was used to introduce the laser beam into the microscope. The fluorescence from the sample excited by randomly polarized light was passed through a 488 nm long-pass filter (Semrock) and detected by a microchannel plate photomultiplier tube (PMT) (R3809U-07, Hamamatsu Photonics). A fast TCSPC board (Becker-Hickl, SPC-830) was used to obtain the fluorescence decay profile. The instrument response function (IRF) of the system was approximately 150 ps. The fluorescence lifetimes were extracted from the measured decay curves by a nonlinear least-squares fit with deconvoluting IRF.

RESULTS AND DISCUSSION

Donor. Coumarin dyes have been modified by attaching a diethylamino group, which acts as an electron donor, to enhance their spectroscopic properties. Upon photoexcitation, diethylaminocoumarins form a twisted intramolecular charge transfer (TICT) state.[16−18] The TICT formation accompanies a fast internal rotation around the C−N bond, which is sensitive to solvent polarity, pH, viscosity, etc. Although those properties are useful when the dyes are applied as environment-sensitive sensors, the TICT formation significantly deteriorates the fluorescence quantum yields of the nonrigid coumarin derivatives. For example, the decrease in fluorescence intensity of a coumarin dye was ten times greater in water than in ethanol.[19]

The TICT process can be blocked by fixing the electron-donating amino group with the rigid julolidine structure. As shown in Figure 1, C334, which was used in this study, belongs

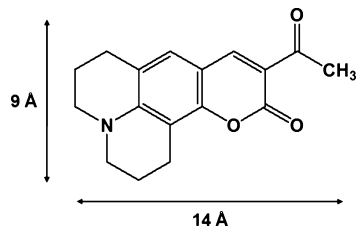

Figure 1. Molecular structure and dimension of coumarin 334.

to one of the rigidified coumairns. Together with the carbonyl group at the 2-position, the acetyl group at the 3-position also acts as the electron acceptor. The axial diameters of C334 are 9 and 14 Å, respectively, with a molecular volume of 252 Å^3.[20] The transition dipole moment of C334 for the $S_1 \leftarrow S_0$ excitation lies along the long axis. Figure 2 shows the fluorescence decay of C334 in water. It is a single exponential with the fluorescence lifetime of 3.6 ns. The radiative decay rate constant (k_r) of C334 was calculated from the absorption and emission spectra (inset in Figure 3) using the Strickler−Berg formula. The calculated k_r value of 2.54×10^8 s^{-1} was used to calculate the quantum yield of C334 ($Q = 0.92$). It is very close to the reported value of 0.87.[21]

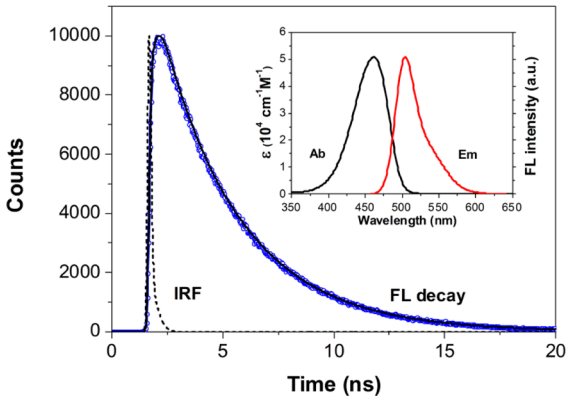

Figure 2. Fluorescence decay profile of C334 in water together with the instrument response function (IRF). The inset shows the absorption and emission spectra of the dye.

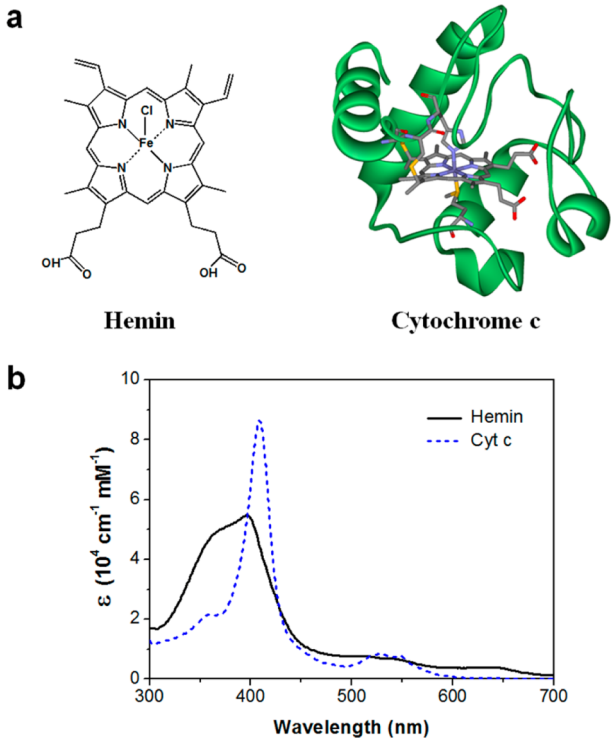

Figure 3. Molecular structures of hemin and cyt *c*. Cyt *c* contains a heme molecule encapsulated by a peptide chain (a). Absorption spectra of hemin (black solid line) and cyt *c* (blue dashed line) in water solution (b).

Acceptors. We have chosen two biologically important molecules as acceptors (Figure 3a). Hemin functions as a heme oxygenase-1 inducer, ion channel stimulator, and intracellular messenger with antiapoptotic and anti-inflammatory properties. Cyt *c* catalyzes several oxidation−reduction reactions in mitochondria through electron transfer between two redox states. The prosthetic group in such a redox protein shows distinct absorption spectra, depending on the redox states, which has recently been utilized as a FRET sensor.[22,23] Figure 3b shows the absorption spectra of hemin and cyt *c* in water. Although hemin is originated from heme, its absorption spectrum is distinct due to the different coordinating ligands to the metal ion. Hemin has a broad absorption band in the 300−450 nm range with a high molar extinction coefficient (λ_{max} = 400 nm) and a tail absorption spanning the 450−700 nm range with a relatively low molar extinction coefficient. In bovine heart cyt *c*, the 6-coordinated Fe^{3+} ion has two biaxial ligands, histidine (H18) and methionine (M80) residues. The oxidized form of cyt *c* that we have used shows the Soret band peak at 410 nm while the Q-bands (α and β) are merged into a single broad absorption peak (11 400 M^{-1} cm^{-1} at 530 nm). Previous spectroscopic results show that heme acts as either a linear or a planar absorber, depending on the absorption wavelength.[24,25] In the UV region (200−380 nm), it is a linear absorber. In the Soret and Q-band region, it is a circular absorber. When the wavelength is longer than 558 nm, it is an elliptical absorber. The fluorescence emission of C334 lies in the range of 475−600 nm. Therefore, the heme of cyt *c* can be regarded as a planar absorber for the C334 emission. In other words, two transition dipoles on the heme plane are mutually orthogonal, which enables the orientation factor to be less sensitive in the energy-transfer process.[26]

Förster Radius. The energy-transfer efficiency is defined as

$$E = \frac{k_T}{k_D + k_T} = 1 - \frac{\tau_{DA}}{\tau_D} \quad (3)$$

Förster radius (R_0) is the distance at which the energy-transfer efficiency is 50%, or the fluorescence lifetime of the donor in the presence of the acceptor is decreased by one-half. R_0 (Å) is related to the spectral properties of the chromophores by[27]

$$R_0 = 0.211(\kappa^2 n^{-4} Q_D J(\lambda))^{1/6} \quad (4)$$

where n is the refractive index of the medium and Q_D is the quantum yield of the donor in the absence of an acceptor, κ^2 is the orientation factor, and $J(\lambda)$ is the spectral overlap between the donor emission and the acceptor absorption, which is given by

$$J(\lambda) = \frac{\int_0^\infty F_D(\lambda)\varepsilon_A(\lambda)\lambda^4 \, d\lambda}{\int_0^\infty F_D(\lambda) \, d\lambda} \quad (5)$$

The formula indicates that the higher R_0 value results from a greater spectral overlap between the donor emission and the acceptor absorption, a higher molar extincition coefficient of acceptor, and a longer wavelength transition of the chromophores.

The orientation factor, as the name implies, is related to the relative orientations of the donor and the acceptor. It can be calculated by the following equation

$$\kappa^2 = (\cos\theta_{DA} - 3\cos\theta_D \cos\theta_A)^2 \quad (6)$$

where θ_{DA} is the angle between the two dipoles and θ_D and θ_A are the angles formed between the donor and acceptor dipoles and the vector connecting them, respectively. The orientation factor lies in the range from 0 to 4 and could be time-dependent if the fluorophores are mobile during the time scale of the energy-transfer process. The R_0 value was calculated with the ensemble averaged κ^2 value of 2/3. This value is usually adopted when there is no a priori knowledge of the spatial distribution of D and A. The R_0 value of the donor and each acceptor pair was calculated using the absorption spectra of the acceptors in solution, which gives rise to 42.8 Å for hemin and 41.5 Å for cyt *c*. For the ensemble system, we have measured that donors and acceptors are fixed in a rigid medium (the static averaging limit). Then, the *b* value in eq 2 should be multiplied by 0.84, as the R_0 is calculated with κ^2 = 2/3.[3]

dx.doi.org/10.1021/jp306164a | J. Phys. Chem. B 2012, 116, 11857−11862

Fluorescence Resonance Energy Transfer. Figure 4a shows the absorption spectra of two acceptors in a PAA

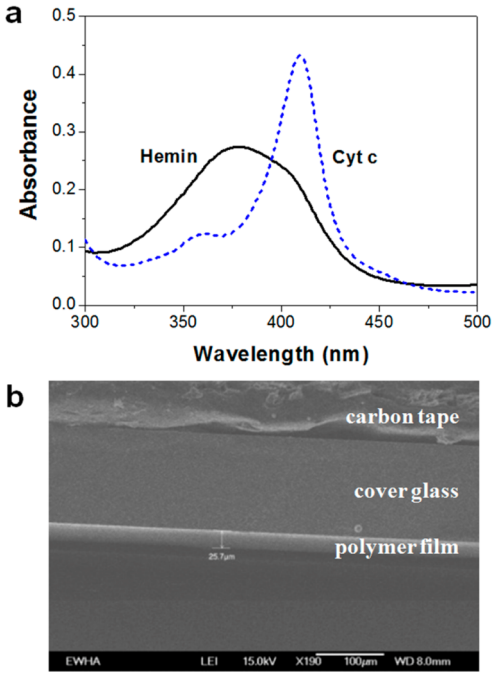

Figure 4. Absorption spectra of hemin (black solid line) and cyt *c* (blue dashed line) in PAA film. SEM image of a polymer thin film used to measure the thickness which shows carbon tape, cover glass, and PAA film as individual layers (b).

polymer film in the 300−500 nm region. The absorption spectrum of cyt *c* is similar to that in aqueous solution, but that of hemin exhibits a significant change. This result indicates that cyt *c* maintains a native form in the PAA matrix while the molecular structure of hemin undergoes a significant distortion. The absorption spectra were merely used to calculate the acceptor concentration without further detailed analysis because it was not the main theme of this work. The thickness of the sample was measured using SEM (Figure 4b), and the acceptor concentration was calculated using Beer's law in which the absorbance was monitored at 375 nm for hemin and 410 nm for cyt *c*. The concentration of hemin was varied from 0 to 23.0 mM and that of cyt *c* from 0 to 9.3 mM. Then, the fluorescence decay profiles of each sample were recorded at known concentrations.

Figure 5 shows the fluorescence decay curves of C334 at different acceptor concentrations of hemin (a) and cyt *c* (b) in PAA films. The fluorescence lifetimes of C334 in PAA films at 0 mM acceptors are different for the (a) and (b) matrices, owing to different pH values. As stated earlier, eq 2 is not adequate because it is a result of an integration ranging from zero to infinity. Moreover, it is not possible to find a functional form that satisfactorily describes the intensity decay profile as a function of time. Therefore, we have attempted to compare the decay time constants for hemin and cyt *c*, which have distinct molecular structures. For this purpose, the data that are not monoexponential were fitted to a multiexponential form to obtain the average lifetimes that represent characteristic time constants. The average lifetime $\langle\tau\rangle$ is defined as

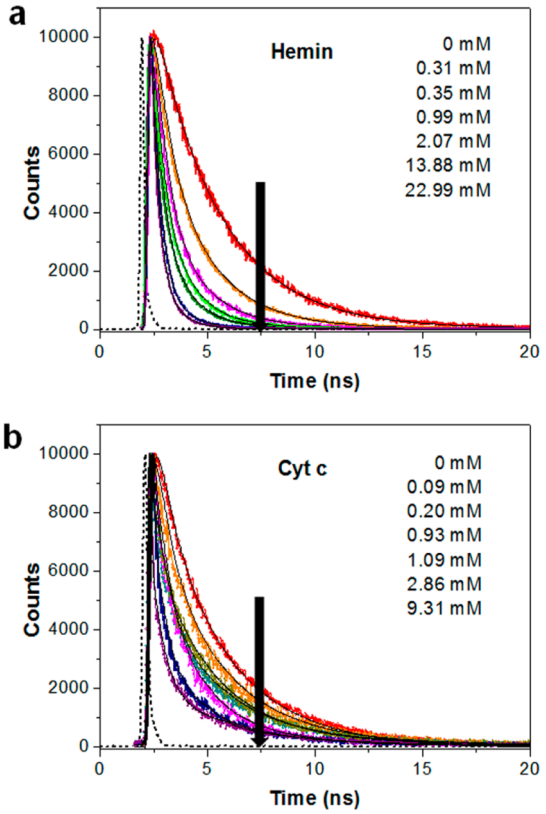

Figure 5. Fluorescence decay profiles of C334 in the presence of hemin in PAA (a). The fluorescence decay profiles of C334 in the presence of cyt *c* in PAA (b).

$$\left\langle \tau \right\rangle = \sum_i \alpha_i \tau_i / \sum_i \alpha_i \tag{7}$$

where α and τ are the amplitude and lifetime component, respectively.[28]

Table 1 shows the average lifetimes of C334 in the presence of hemin and cyt *c* at different concentrations. Then, the

Table 1. Average Fluorescence Lifetime of the Donor and the Average Distance between C334 and Hemin or Cyt *c* in PAA Films

hemin (mM)	$\langle\tau\rangle$ (ns)	$\langle r\rangle$ (Å)	cyt *c* (mM)	$\langle\tau\rangle$ (ns)	$\langle r\rangle$ (Å)
0	3.04	–	0	2.62	–
0.31	1.04 ± 0.08	38.4	0.09	2.19 ± 0.05	54.4
0.35	1.77 ± 0.12	45.2	0.20	1.82 ± 0.09	47.6
0.99	0.67 ± 0.04	34.7	0.93	1.27 ± 0.27	41.1
2.07	0.85 ± 0.03	36.5	1.09	1.60 ± 0.49	45.2
13.88	0.36 ± 0.14	30.5	2.86	1.05 ± 0.33	38.8
22.99	0.28 ± 0.13	29.0	9.31	1.06 ± 0.35	38.9

average distance $\langle r\rangle$ at the given acceptor concentration was calculated through the well-known FRET equation:

$$k_T = \frac{1}{\tau_{DA}} - \frac{1}{\tau_D} = \frac{1}{\tau_D}\left(\frac{R_0}{r}\right)^6 \tag{8}$$

Figure 6 shows the plot of $\langle r\rangle$ as a function of acceptor (hemin and cyt *c*) concentration. When the acceptor concentration is low (<5 mM), they show very similar behavior. When the

dx.doi.org/10.1021/jp306164a | J. Phys. Chem. B 2012, 116, 11857−11862

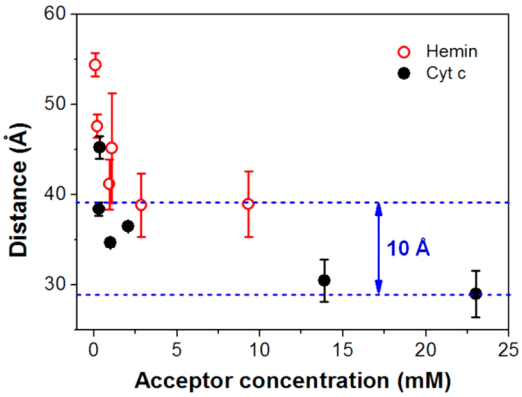

Figure 6. Distances between donors and acceptors, showing the 10 Å differences between the D−A distances of each pair when they appear to be constant at a certain acceptor concentration.

acceptor concentration is high (>5 mM), there exists a significant difference. As concentration increases, the distances between donor and acceptor converge to 31 Å for hemin and 41 Å for cyt *c*, which make a difference of 10 Å.

We have used a very low concentration of donors, thus making the homotransfer between donors negligible. This is the situation where well-separated donors are surrounded by many randomly distributed acceptors. When a high concentration of acceptors is used, energy transfer among acceptors is possible. This problem can be resolved by using acceptors of ulftrafast lifetime. The excited-state decay of heme is in the range of a few picoseconds or less[29−31] and thus the energy transfer between acceptors is unlikely to occur. Therefore, we can focus only on the D−A energy-transfer process. Blumen and Manz theoretically analyzed the effect of the finite sizes of chromophores,[32] which Förster did not consider in his introductory FRET model. They introduced a cutoff parameter that represents the effect and solved the equation numerically. Klafter and Blumen further refined the model to include more general cases of restricted geometries.[33] Their work has drawn considerable interest and is still in use today.[34−38] Accommodating the finite sizes of D, A, and the film thickness in three-dimensional space, the intensity decay profile of a donor in the presence of many acceptors can be written in the continuum approximation:

$$I(t) = \exp\left[-\frac{t}{\tau_0} - p\int_{\alpha}^{\beta}(1 - \exp[-tw(r)])4\pi\rho(r)r^2\,\mathrm{d}r\right] \quad (9)$$

where p is the probability of occupying a site by the acceptors, $w(r)$ is the donor−acceptor interaction term, and $\rho(r)$ is the site density function which is inversely proportional to the number of acceptors per site (lattice) volume.[32,33] One can simply assume the dipole−dipole interaction and homogeneous distribution of acceptors. In this case, the ρ is constant and $p\rho$ is nothing other than the number density. The minimum α value should be the sum of the donor and acceptor radii. Apparently, the α value is very different for C334−hemin and C334−cyt *c* pairs. The β value depends on the geometrical structure of the system of interest. The parameter plays an important role when FRET occurs in the restricted geometries. In the case of the polymer thin films, the β value is limited by the film thickness (d). When the $d \gg R_0$, then the upper limit can be taken as infinity.

Excluded Volume Effect. Tcherkasskaya et al. have first attempted to theoretically describe the matter of the excluded volume effect in FRET.[39] Their results showed that the time dependence of the donor decay in the presence of high acceptor content is quite complex and does not follow the stretched exponential model. In more detail, it showed two distinct temporal behaviors, and the crossover between those regimes depends on spatial confinements in molecular distributions. Bojarski and co-workers have solved the problem by performing Monte Carlo simulations under conditions of low donor and high acceptor concentrations.[40] The results indicate that the inclusion of the excluded volume effect lengthens the average lifetime of the decay profiles. Obviously, the effect became more pronounced as the cavity radius and concentration increased.

As shown in Figure 6, the excluded volume effect is much more pronounced in cyt *c* compared with hemin. The radius of hemin has been reported as 6 Å[41] and that of cyt *c* was considered to be 16 Å from measurements via SAXS[42] and fluorescence correlation spectroscopy,[43] which may account for the origin of the 10 Å difference in the average distance between hemin and cyt *c*. Figure 7 shows the excluded volume

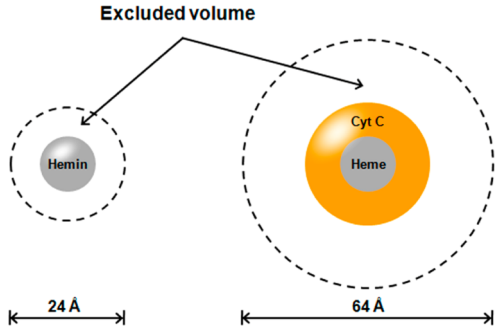

Figure 7. Schematic depiction of the exclude volume effect. The individual dotted line indicates the diameter of the excluded volume that becomes 4 times the molecular radius. Polypeptide chains enhance the effect by causing the overlaps as observed in cyt *c*.

in which the overlapping configuration of cyt *c* is impossible due to the polypeptide chain. Therefore, the effect of hemin should occur at a much higher concentration than 23 mM because cyt *c* is a structure in which the heme is encapsulated by apoprotein. Our observations clearly indicate that the use of the stretched exponential model (eq 2) is severely limited in the case of sizable acceptors at high concentration due to the excluded volume. We think the effect should be seriously considered in the interpretation of FRET data, especially when bulk chromophores are used.

CONCLUSIONS

Förster first presented an analytical solution for the energy-transfer process in an ensemble system in which donors and acceptors are randomly distributed in matrix. Although the equation is quite successful at low and moderate acceptor concentrations, it is problematic at the high concentration limit because the equation was derived without considering the excluded volume. In this work, the effect was investigated using time-resolved FRET. We used C334 as the energy donor and hemin and cyt *c* as the acceptors and measured the intensity decays of C334 surrounded by a number of acceptors in poly(acrylic acid) . When the acceptor concentration is low (<5

dx.doi.org/10.1021/jp306164a | J. Phys. Chem. B 2012, 116, 11857−11862

mM), both acceptors show very similar behavior. However, when the acceptor concentrations are high (>5 mM), the excluded volume effect is much more pronounced in cyt *c* compared with hemin. At the high-concentration limit, the comparative molecular sizes of hemin and cyt *c* result in the different plateau value of 10 Å. This is because the excluded volume in which the overlapping configuration of cyt *c* is impossible due to the polypeptide chain. Our results support previous theoretical and computational studies on the related FRET work, and we conclude that the excluded volume effect should be primarily considered when the chromophore is a part of the acceptor like cyt *c*.

AUTHOR INFORMATION

Corresponding Author

*E-mail: mylee@ewha.ac.kr.

Notes

The authors declare no competing financial interest.

ACKNOWLEDGMENTS

This work was supported by the Basic Science Research Program (2010-0541-2), the Acceleration Research Program through the National Research Foundation of Korea, and the Global Top5 Grant of Ewha Womans University.

REFERENCES

(1) Förster, T. *Z. Naturforsch., A* **1949**, *4*, 321−347.
(2) Valeur, B.; Berberan-Santos, M. In *Molecular Fluorescence*, 2nd ed.; Wiley-VCH: Weinheim, Germany, 2012.
(3) Lee, M.; Tang, J.; Hochstrasser, R. M. *Chem. Phys. Lett.* **2001**, *344*, 501−508.
(4) Yang, S.; Cao, J. *J. Chem. Phys.* **2004**, *121*, 562−571.
(5) Felorzabihi, N.; Froimowicz, P.; Haley, J. C.; Bardajee, G. R.; Li, B.; Bovero, E.; van Veggel, F.; Winnik, M. A. *J. Phys. Chem. B* **2009**, *113*, 2262−2272.
(6) Colby, K. A.; Burdett, J. J.; Frisbee, R. F.; Zhu, L.; Dillon, R. J.; Bardeen, C. J. *J. Phys. Chem. A* **2010**, *114*, 3471−3482.
(7) Nemkovich, N. A.; Reis, H.; Baumann, W. *J. Lumin.* **1997**, *71*, 255−263.
(8) Ramakrishna, G.; Ghosh, H. N. *J. Phys. Chem. A* **2002**, *106*, 2545−2553.
(9) Zhang, X.; Guo, L.; Wu, F.-Y.; Jiang, Y.-B. *Org. Lett.* **2003**, *5*, 2667−2670.
(10) Hara, K.; Sato, T.; Katoh, R.; Furube, A.; Ohga, Y.; Shinpo, A.; Suga, S.; Sayama, K.; Sugihara, H.; Arakawa, H. *J. Phys. Chem. B* **2003**, *107*, 597−606.
(11) Wang, Z.-S.; Cui, Y.; Hara, K.; Dan-oh, Y.; Kasada, C.; Shinpo, A. *Adv. Mater.* **2007**, *19*, 1138−1141.
(12) Kim, M. H.; Jang, H. H.; Yi, S.; Chang, S.-K.; Han, M. S. *Chem. Commun.* **2009**, 4838−4840.
(13) Li, H.; Cai, L.; Li, J.; Hu, Y.; Zhou, P.; Zhang, J. *Dyes Pigm.* **2011**, *91*, 309−316.
(14) Porel, M.; Klimczak, A.; Freitag, M.; Galoppini, E.; Ramamurthy, V. *Langmuir* **2012**, *28*, 3355−3359.
(15) Soto-Ortega, D. D.; Murphy, B. P.; Gonzalez-Velasquez, F. J.; Wilson, K. A.; Xie, F.; Wang, Q.; Moss, M. *Bioorg. Med. Chem.* **2011**, *19*, 2596−2602.
(16) Taneja, L.; Sharma, A. K.; Singh, R. D. *J. Lumin.* **1995**, *63*, 203−214.
(17) Satpati, A. K.; Kumbhakar, M.; Nath, S.; Pal, H. *Photochem. Photobiol.* **2009**, *85*, 119−129.
(18) Tablet, C.; Matei, I.; Pincu, E.; Meltzer, V.; Hillebrand, M. *J. Mol. Liq.* **2012**, *168*, 47−53.
(19) Gupta, M.; Maity, D. K.; Singh, M. K.; Nayak, S. K.; Ray, A. K. *J. Phys. Chem. B* **2012**, *116*, 5551−5558.
(20) Dutt, G. B.; Ghanty, T. K. *J. Phys. Chem. B* **2003**, *107*, 3257−3264.
(21) Arici, E.; Raubacher, F.; Wendorff, J. H. *Macromol. Chem. Phys.* **2000**, *201*, 1679−1686.
(22) Li, B.; Qin, C.; Li, T.; Wang, L.; Dong, S. *Anal. Chem.* **2009**, *81*, 3544−3550.
(23) Sharon, E.; Freeman, R.; Willner, I. *Anal. Chem.* **2010**, *82*, 7073−7077.
(24) Eaton, W. A.; Hochstrasser, R. M. *J. Chem. Phys.* **1967**, *46*, 2533−2539.
(25) Churg, A. K.; Makinen, M. W. *J. Chem. Phys.* **1978**, *68*, 1913−1925.
(26) Caesar, C.; Esbjorner, E. K.; Lincoln, P.; Norden, B. *Biophys. J.* **2009**, *96*, 3399−3411.
(27) Lakowicz, J. R. *Principles of Fluorescence Spectroscopy*, 3rd ed.; Springer: New York, 2006.
(28) Jee, A.-Y.; Bae, E.; Lee, M. *J. Phys. Chem. A* **2009**, *113*, 16508−16512.
(29) Wang, W.; Ye, X.; Demidov, A. A.; Rosca, F.; Sjodin, T.; Cao, W.; Sheeran, M.; Champion, P. M. *J. Phys. Chem. B* **2000**, *104*, 10789−17801.
(30) Negrerie, M.; Cianetti, S.; Vos., M. H.; Martin, J. L.; Kruglik, S. G. *J. Phys. Chem. B* **2006**, *110*, 12766−12781.
(31) Bram, O.; Consani, C.; Cannizzo, A.; Chergui, M. *J. Phys. Chem. B* **2011**, *115*, 13723−13730.
(32) Blumen, A.; Manz, J. *J. Chem. Phys.* **1979**, *71*, 4694−4702.
(33) Blumen, A.; Klafter, J.; Zumofen, G. *J. Chem. Phys.* **1986**, *84*, 1397−1401.
(34) Yekta, A.; Winnik, M. A.; Farinha, J. P. S.; Martinho, J. M. G. *J. Phys. Chem. A* **1997**, *101*, 1787−1792.
(35) Rolinski, O.; Birch, D. J. S. *J. Chem. Phys.* **2002**, *112*, 8923−8927.
(36) Farinha, J. P. S.; Spiro, J. G.; Winnik, M. A. *J. Phys. Chem. B* **2004**, *108*, 16392−16400.
(37) Farinha, J. P. S.; Martinho, J. M. G. *J. Phys. Chem. C* **2008**, *112*, 10591−10601.
(38) Hilczer, M.; Tachiya, M. *J. Chem. Phys.* **2009**, *130*, 184502−184507.
(39) Tcherkasskaya, O.; Gronenborn, A. M.; Klushin, L. *Biophys. J.* **2002**, *83*, 2826−2834.
(40) Rangelowa-Jankowska, S.; Kulak, L.; Bojarski, P. *Chem. Phys. Lett.* **2008**, *460*, 306−310.
(41) Dickerson, R. E.; Geis, I. *Hemoglobin: Structure, Function, Evolution and Pathology*; Benjamin/Cummings: Menlo Park, CA, 1983.
(42) Akiyama, S.; Takahashi, S.; Kimura, T.; Ishimori, K.; Morishima, I.; Nishikawa, Y.; Fujisawa, T. *Proc. Natl. Acad. Sci. U.S.A.* **2002**, *99*, 1329−1334.
(43) Werner, J. H.; Joggerst, R.; Dyer, R. B.; Goodwin, P. M. *Proc. Natl. Acad. Sci. U.S.A.* **2006**, *103*, 11130−11135.